Gaussian process for calibration and control of the GlueX Central Drift Chamber

T Britton, D McSpadden, T Jeske, N Kalra, and D Lawrence
Thomas Jefferson National Accelerator Laboratory, Newport News, VA 23606, USA

N Jarvis
Carnegie Mellon University, Pittsburgh, PA 15213, USA

Abstract. We have developed and implemented a machine learning-based system to calibrate and control the GlueX Central Drift Chamber at Jefferson Lab, VA, in near real-time. The system monitors environmental and experimental conditions during data taking and uses those as inputs to a Gaussian process (GP) with learned prior. The GP predicts calibration constants in order to recommend a high voltage (HV) setting for the detector that maintains consistent detector performance (gain and resolution) throughout data taking. This approach is in stark contrast to traditional detector operations in which the detector operates at fixed HV and its calibration parameters vary quite considerably with time. Additionally, the ML-based system utilizes uncertainty quantification to correct the recommended control parameters when appropriate. We will present results from the ML system running autonomously during the Charged Pion Polarizability (CPP) experiment conducted in Hall D at Jefferson Lab.

1. Introduction

The GlueX experiment is housed in Jefferson Lab's newest experimental hall, Hall D, and is designed to search for exotic hybrid mesons via photoproduction[1]. The GlueX spectrometer is comprised of several tracking detectors and calorimeters, including the Central Drift Chamber (CDC) [2], which is a gas-filled tracking detector for charged particles.

Data gathered from the detector must be calibrated in order to be useful in subsequent physics research. The CDC has two calibrations: a gain correction factor (GCF) and a drift time calibration. This work focuses on the GCF, which has a variation of $\pm 15\%$. The CDC has only one control: the operating voltage of the detector.

Traditionally the CDC is operated at a fixed high voltage (2125 V) with calibration performed on the data as a post-processing step. The calibration process is iterative, computationally expensive, and occurs after data taking; delaying subsequent physics analysis. With artificial intelligent systems, the high voltage (HV) of the CDC could be changed as needed to stabilize the GCF of the CDC thus eliminating the need for such expensive calibrations. This is the main motivation for the research presented.

1.1. Can we predict GCFs?

Before we can enact controls for the CDC, we need to accurately predict the GCFs using the conditions in which the detector is operated. By accurately predicting the GCF and knowing

the relationship between HV and gain we can, in principle, adjust the HV to counteract changes in GCF. To begin the process of predicting the GCF our detector expert identified variables likely to influence the detector's GCF.

After initial analysis 3 variables were chosen as having the largest impact on CDC GCF. The variables are: the atmospheric pressure, the temperature of the Ar:CO_2 gas mixture which fills the CDC, and the current drawn from the CDC HV boards (a proxy for charged particle flux). It is encouraging that these variables appeared to have the highest correlation as they agreed with literature of drift chamber design and operation[3]. During data taking, the input features are readily available from the Experimental Physics Industrial Controls System (EPICS), are not dependent on other detectors, and do not require event reconstruction (a slow, computationally intensive process not feasible for use in a real-time environment).

After initial studies and testing, a Gaussian Process (GP) was selected as the machine learning (ML) technique to best accomplish the goal of predicting CDC GCFs. A GP with a single output parameter infers a latent function $R^p \rightarrow R$, to map training input X and corresponding targets y [4]. X is the matrix of N observations of the selected features, $x_n \in R^p$, and n is the n^{th} observation and p is the number of features, in our case three. The mapping uses a selected covariance function, $k(x, x')$, to control the smoothness of the mapping output from one training point to the next closest training point [5]. In our case, $k(\cdot, \cdot)$ is a **sum** kernel of Scikit-learn's [6] Radial Basis Function (RBF), as shown in Eq. 1, and White Noise (WN), as shown in Eq. 2. The RBF explains the covariance of the data, where l is the learned length scale parameter used to scale the difference in distance between training observations.

$$k_{RBF}(x, x') = \exp\left(-\frac{(x - x')^2}{2l^2}\right) \tag{1}$$

The WN is used to describe the combined global noise in the data, where σ^2 is the variance of the noise, and I_n is the identity matrix.

$$k_{WN}(x, x') = \sigma^2 I_n, \tag{2}$$

The GP for this application implements the 3 variables listed above as input features with exactly one target value: the GCF of the CDC. Two GPs, one with an Isotropic Radial Basis Function plus white noise and the other with an Anisotropic Radial Basis Function plus white noise, performed well below our goal of a 5% error in predicting the GCF, thus the GP with Isotropic Radial Basis Function was used.

There is a known relationship between GCFs and the operational HV of the CDC, as shown in Figure 1. This relationship can be exploited to recommend a HV setting based on relative signal peak amplitudes, which is influenced by gain.

1.2. Can we control HV to stabilize gain?

On its own the model cannot control the CDC. For that a modular system was developed to gather the needed input variables, feed them into the model, receive the results of inference, convert that inference to a CDC HV setting, and finally, control the CDC. A diagram of the modular system is given in Figure 2.

The system is configurable to allow different modes of operation, from continual operation with fine-grained controls to running on-demand. All system behavior, including hot-swappable models, are configurable on-the fly. The Control System, System Configuration, and model components comprise the core capabilities. The Control System is responsible for interacting with the CDC's HV controls, i.e. translating model recommendations into action. The remaining components provide the model inputs, log system behavior, and provide monitoring capabilities.

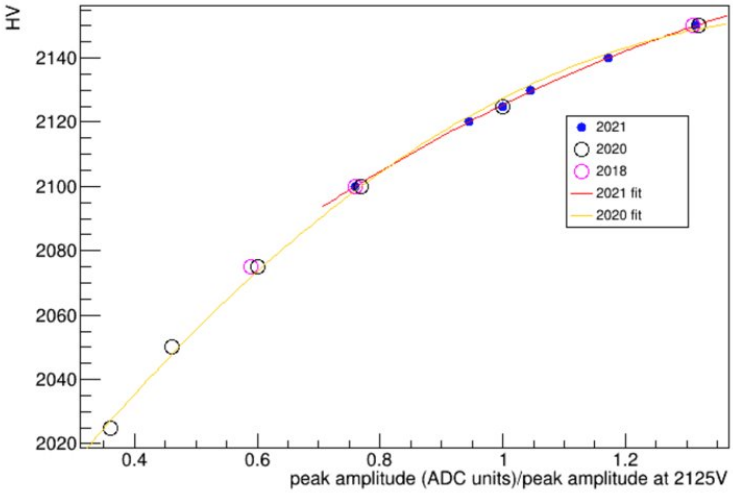

Figure 1. The CDC HV setting versus the relative peak amplitude at a given HV to that at the standard HV setting of 2125V. This relationship is exploited to recommend a HV setting for the CDC given a predicted GCF, which is related directly to the signal peak amplitudes.

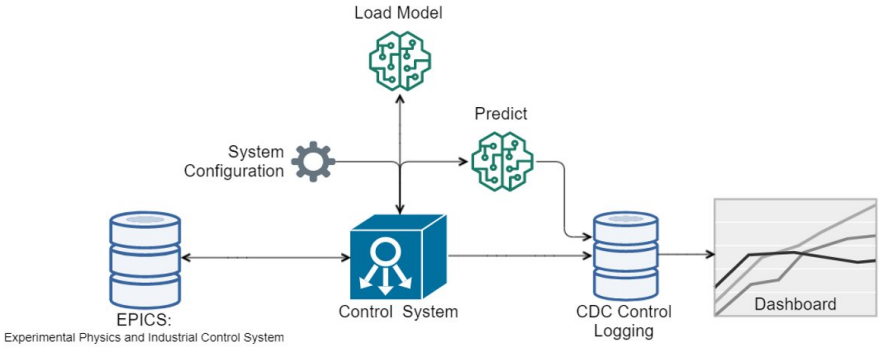

Figure 2. A schematic of the AI based control system showing the model utilities as circuits, the overall system configuration as a cog, and the control system as a cube which takes in values from EPICS and performs control operations while maintaining a comprehensive log of actions.

To aid in ease of running inference with a given model, the model and other necessary parameters are co-located such that only a reference to Tensorflow's Proto-buffer file is needed. The main system utilizes a model utility script which finds and collects the needed files and prepares the model for inference. The system then queries EPICS, performs the necessary preprocessing, and forms a dictionary of input features to be fed to the model via its utility function. The system receives an output dictionary from the model utilities which it then uses to decide how the CDC should be controlled. Should the system decide that the CDC HV should be modified, it passes the settings to another utility which interacts with the controls system and changes the CDC HV.

Before any experimental data was taken, the CDC was divided *via software* into roughly equal "left" and "right" sides in order to test the ability of the control system to stabilize the gain. Cosmic ray data were then taken with one side operating at a fixed 2130 V and the other side controlled by the AI control system, which updated the HV setting of the CDC every 5 minutes.

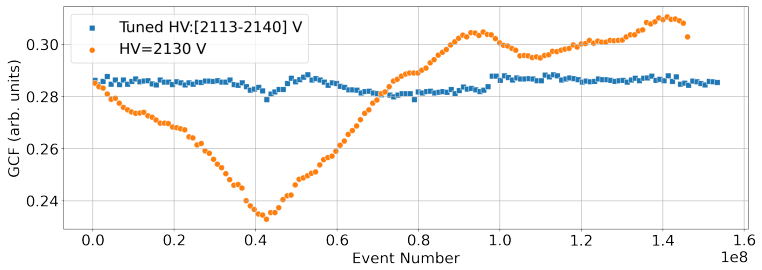

Figure 3. Results of controlling half of the CDC using the AI control system (blue squares) compared to a fixed CDC HV (orange circles) over the Cosmic Ray test (about 2 weeks). This shows an almost order of magnitude decrease in GCF variation when using the AI control system.

During the roughly two weeks of data taking, the system performed as expected, autonomously. After completion of data taking, the GCFs for the two sides were computed. The results can be found in Figure 3. The side controlled by AI is clearly seen to have provided much more stable GCFs (∼3% variation) than the side held at a fixed HV, which saw an almost 30% variation over the same time period.

2. Trust and Uncertainty Quantification: Does the system generalize to Other Running Conditions?

One clear advantage of using a Gaussian Process is the inherent uncertainty quantification (UQ) it provides. Any system trusted with the operation of a sophisticated tracking detector must be trustworthy. This UQ is an indication of the model's confidence in its prediction/recommendations, how similar the current operational environment is to the data the model was trained with. Typically, naive models will revert to their means when they get far enough outside of their training regime. There are methods, which were employed here, to help aid the transition from operational regions covered by training data to those not covered, but still there remain cases where the CDC will operate outside of regions of model confidence. To alleviate this concern, a confidence threshold was selected and a corresponding surface in input feature space was established. This surface is dependent on the selection of a threshold; examples of how the surface varies with differing thresholds can be seen in Figure 2. An uncertainty threshold of 3% was determined to provide the correct balance model coverage in feature space and GCF resolution. Thus the result of inference can either exist inside the volume contained by the surface or exist outside of the surface. Each class of inference results is then independently handled. For inside results, the predicted GCFs are used to derive the recommended HV setting. Outside results are subjected to a UQ correction protocol. For the results presented here, this protocol projects the 3-dimensional input point (input pressure, input temperature, input high voltage board current) onto the surface. This corrected point then became the basis for the inference of the GCF, which in turn was used to compute a recommended HV setting.

2.1. Charged Pion Polarizability Tests

The above UQ correction was exercised during the Charged Pion Polarizability (CPP) experiment which ran with a substantially lower luminosity than GlueX, the experiment whose data was used to train the model used by the system. This is well evident in Figure 5 which shows the vast majority of data taken was taken outside of the confidence surface. Additionally, HV control was only done once at the start of each run (a roughly 2hr block of data taking) due to other constraints present in data taking. Even with this being true, and a widely varying

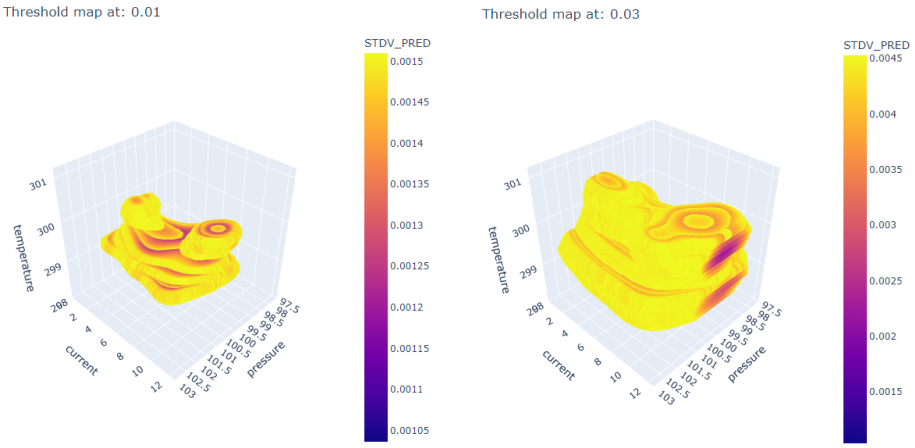

Figure 4. Images showing the confidence surface for a threshold of 0.01 (left) and the chosen threshold of 0.03 (right).

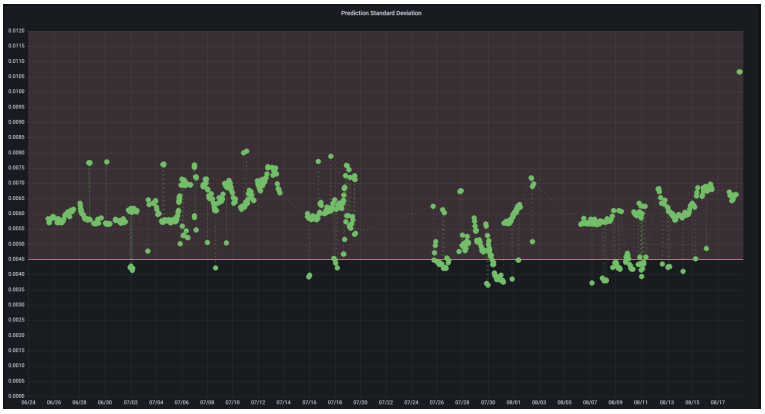

Figure 5. A plot of prediction standard deviation versus time for the CPP program (about two months). A point in the top red shaded area indicates a point outside of the confidence threshold surface which caused the UQ correction protocol to be invoked.

atmospheric pressure (see fig. 6), the AI system was able to robustly operate outside of the training region, providing a stabilized GCF.

3. Conclusion

To accomplish this, a control system was developed which integrates the already present EPICS and a Gaussian process to accurately control the GlueX CDC in near real-time. The system takes a prediction for the GCF and exploits a known relationship between GCF and HV setting to counteract changes in GCF with changes in CDC HV settings. The system is uncertainty aware enabling it to robustly control the CDC in the face of novel operational conditions. Thus far the system has been successfully deployed in cosmic ray testing, where it demonstrated almost an order of magnitude decrease in GCF variation, and in the CPP experiment where it likewise stabilized the GCF. With these successes, the AI control system has become part of the standard operation of the CDC, and its continued development has made it more flexible and robust in operation.

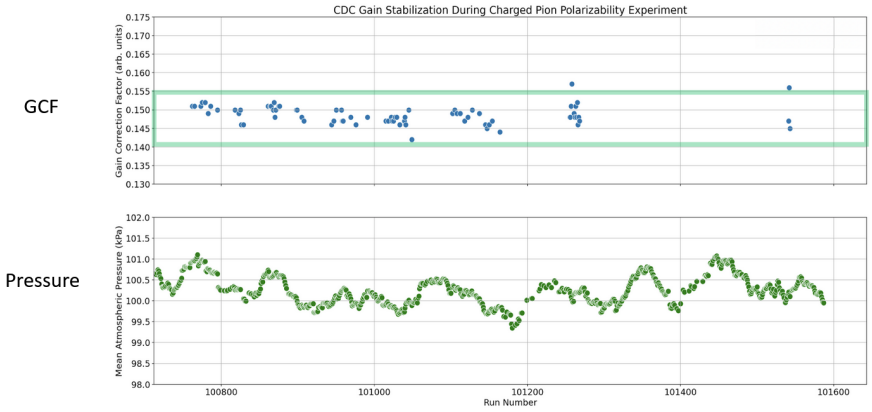

Figure 6. Plots showing GCF stabilization during the CPP experiment. The top plot shows the predicted GCF along with the desired 5% bounding box. The bottom plot shows the atmospheric pressure (the biggest driver of GCF) over the same period of time.

4. Acknowledgments

Jefferson Science Associates, LLC operated Thomas Jefferson National Accelerator Facility for the United States Department of Energy under U.S. DOE Contract No. DE-AC05-06OR23177.

This work was supported by the US DOE as LAB 20-2261.

The Carnegie Mellon Group is supported by the U.S. Department of Energy, Office of Science, Office of Nuclear Physics, DOE Grant No. DE-FG02-87ER40315.

GlueX acknowledges the support of several funding agencies and computing facilities: www.gluex.org/thanks.

References

[1] S. Adhikari et al. The GlueX beamline and detector. *Nuclear Instruments and Methods in Physics Research Section A: Accelerators, Spectrometers, Detectors and Associated Equipment*, 987:164807, jan 2021. https://doi.org/10.1016/j.nima.2020.164807 doi:10.1016/j.nima.2020.164807.

[2] N.S. Jarvis, C.A. Meyer, B. Zihlmann, M. Staib, A. Austregesilo, F. Barbosa, C. Dickover, V. Razmyslovich, S. Taylor, Y. Van Haarlem, G. Visser, and T. Whitlatch. The Central Drift Chamber for GlueX. *Nuclear Instruments and Methods in Physics Research Section A: Accelerators, Spectrometers, Detectors and Associated Equipment*, 962:163727, may 2020. https://doi.org/10.1016/j.nima.2020.163727 doi:10.1016/j.nima.2020.163727.

[3] Fabio Sauli. Principles of Operation of Multiwire Proportional and Drift Chambers. page 92 p, Geneva, 1977. CERN, CERN. CERN, Geneva, 1975 - 1976. URL: https://cds.cern.ch/record/117989, https://doi.org/10.5170/CERN-1977-009 doi:10.5170/CERN-1977-009.

[4] Carl Edward Rasmussen, Christopher KI Williams, et al. *Gaussian processes for machine learning*, volume 1. Springer, 2006.

[5] David Barber. *Bayesian Reasoning and Machine Learning*. Cambridge University Press, 2012.

[6] F. Pedregosa, G. Varoquaux, A. Gramfort, V. Michel, B. Thirion, O. Grisel, M. Blondel, P. Prettenhofer, R. Weiss, V. Dubourg, J. Vanderplas, A. Passos, D. Cournapeau, M. Brucher, M. Perrot, and E. Duchesnay. Scikit-learn: Machine learning in Python. *Journal of Machine Learning Research*, 12:2825–2830, 2011.